Journal of Marine Science and Technology

Volume 24 | Issue 4 Article 23

PHYSICAL PROPERTY INTERPRETATION OF SEDIMENTS IN THE SOUTHWESTERN SLOPE OF THE ULLEUNG BASIN, EAST SEA, USING DOWNHOLE LOG DATA

Gil Young Kim
Petroleum & Marine Research Division, Korea Institute of Geoscience and Mineral Resources (KIGAM), Daejeon 34132, South Korea., gykim@kigam.re.kr

Dong Geun Yoo
Petroleum & Marine Research Division, Korea Institute of Geoscience and Mineral Resources (KIGAM), Daejeon 34132, South Korea.

Recommended Citation
Kim, Gil Young and Yoo, Dong Geun (2016) "PHYSICAL PROPERTY INTERPRETATION OF SEDIMENTS IN THE SOUTHWESTERN SLOPE OF THE ULLEUNG BASIN, EAST SEA, USING DOWNHOLE LOG DATA," *Journal of Marine Science and Technology*: Vol. 24: Iss. 4, Article 23.
DOI: 10.6119/JMST-016-0420-1
Available at: https://jmstt.ntou.edu.tw/journal/vol24/iss4/23

PHYSICAL PROPERTY INTERPRETATION OF SEDIMENTS IN THE SOUTHWESTERN SLOPE OF THE ULLEUNG BASIN, EAST SEA, USING DOWNHOLE LOG DATA

Acknowledgements

This work was supported by Ministry of Knowledge Economy (MKE) and the Gas Hydrate Research and Development Organization (GHDO) of Korea. We gratefully thank the participants of the UBGH1 Program. This research is affiliated with the K-IODP project, the “International Ocean Discovery Program”, funded by the Ministry of Oceans and Fisheries, Korea

Journal of Marine Science and Technology, Vol. 24, No. 4, pp. 896-904 (2016)
DOI: 10.6119/JMST-016-0420-1

PHYSICAL PROPERTY INTERPRETATION OF SEDIMENTS IN THE SOUTHWESTERN SLOPE OF THE ULLEUNG BASIN, EAST SEA, USING DOWNHOLE LOG DATA

Gil Young Kim and Dong Geun Yoo

Key words: physical properties, log data, Ulleung Basin, sediment, East Sea.

ABSTRACT

This study focuses on the physical properties of two logged sites (UBGH1-1 and UBGH1-14) in the Ulleung Basin, East Sea. Based on seismic profiles, the upper ~50-m layer at logged sites is dominated by turbidite/hemipelagic sediments, whereas the sediments beneath this depth are characterized by thick mass transport deposits (MTDs). Physical property data (velocity, density, porosity, resistivity, and natural gamma) were acquired using Schlumberger's logging tools during logging-while-drilling operations. The variation of physical properties at site UBGH1-1 is likely mostly related to consolidation/compaction effects within typical unconsolidated marine sediment types. Repeated turbidite sequences also affect physical property variability. At site UBGH1-14, density and electrical resistivity log data are elevated and constant, respectively, throughout the MTD. In other words, the physical properties of site UBGH1-14 were likely affected by MTD. The overall relationships among the physical properties at both sites generally correlate, but are affected by some data scattering (at UBGH1-14) and clustering (at UBGH1-1). This is thought to result from the different sediment properties within the mass flow deposits (e.g., turbidite/hemipelagic and MTD). Frequency distributions of each property differ for the two sites. This may be indicative of the differences in the sedimentary environments during deposition and/or after deposition.

I. INTRODUCTION

The physical properties of marine sediments are of great interest in a number of fields such as seafloor engineering, sedimentology, soil mechanics, marine geophysics, and underwater acoustics (Hamilton, 1970, 1980; Hamilton and Bachman, 1982; Richardson et al., 2002; Kim et al., 2007, 2010). They are important factors in understanding past geological events in marine sedimentary environments and in interpreting reflectivity within marine seismic data. Such research is often focused on the relationships between physical and acoustic properties and textural parameters relative to various sedimentary environments.

Downhole logs (e.g., mechanical, radioactive, acoustic, and electrical logs) can be used to distinguish between oil, gas, and water in a reservoir. In addition, downhole log data are used to define physical rock characteristics such as lithology, porosity, pore geometry, and permeability (Asquith and Krygowski, 2004). In particular, acoustic log data can be used to constrain velocity-depth profiles in seismic data collected in the area. In the case of water-saturated marine sediments, electrical resistivity variations reflect changes in porosity and fabric because the conduction of electric currents through sediments depends, in part, on the porosity of the sediments (Asquith and Krygowski, 2004). As a result, electrical resistivity may be considered a lithology indicator for marine sediments.

In 2007 and 2010, the Gas Hydrate Research and Development Organization of Korea acquired logging-while-drilling (LWD) data in the Ulleung Basin, East Sea. Some of the results of gas hydrate investigations using LWD data have been published in previous studies (Kim et al., 2011, 2013). In this study, the downhole log data collected from sites UBGH1-1 and UBGH1-14 (Fig. 1) during 2007 are used to interpret physical properties. The objectives of this study are to present the variability of physical properties with subbottom depth and to establish relationships between the various physical properties that have been measured. In addition, by comparing the physical properties at the two sites, we attempt to interpret and explain their differences.

Paper submitted 10/12/15; revised 03/18/16; accepted 04/20/16. Author for correspondence: Gil Young Kim (e-mail: gykim@kigam.re.kr).
Petroleum & Marine Research Division, Korea Institute of Geoscience and Mineral Resources (KIGAM), Daejeon 34132, South Korea.

II. GEOLOGIC SETTING

The Ulleung Basin of the East Sea is a bowl-shaped back-arc

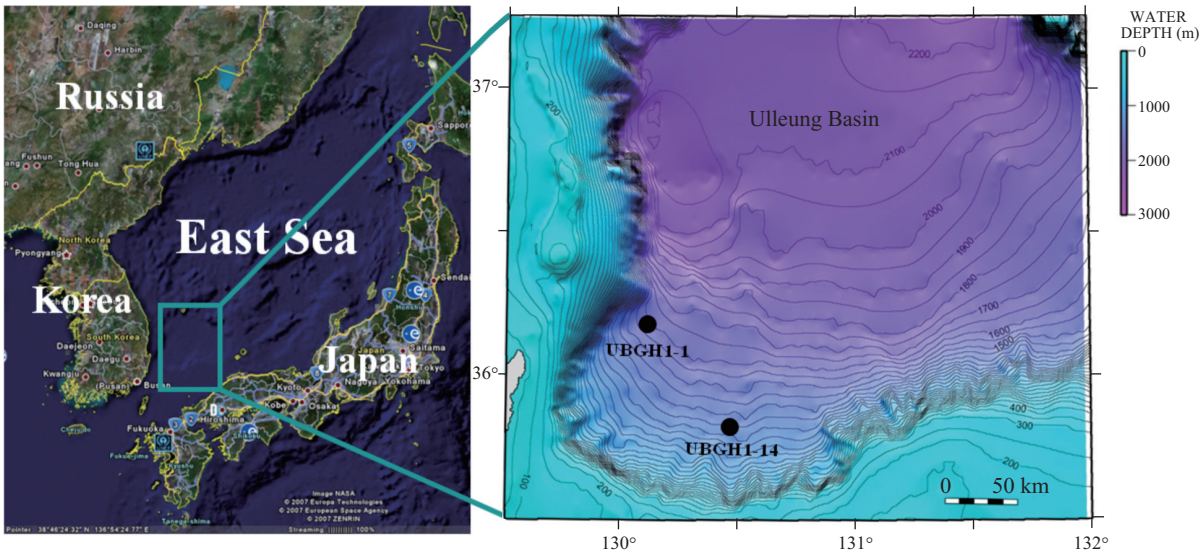

Fig. 1. Physiographic map of the East Sea. The box represents the Ulleung Basin shown on the right side. Two drilling sites are marked in right figure. Water depths of sites UBGH1-1 and UBGH1-14 are 1445 and 1354 m, respectively. Contours are in meters.

basin (Fig. 1). The basin is bounded by the continental slopes of the Korean Peninsula, the Korea Plateau, the Oki Bank, and the Japanese Arc. Thick Neogene strata, uplifted and faulted by back-arc closure, are present on the southern margin (Lee et al., 1999). The central part of the basin shows fairly smooth seafloor topography that dips gently to the northeast in water depths of 2000-2500 m. The basin contains a relatively undeformed sedimentary section up to 5 km thick, with the acoustic basement in the southern basin lying below ~10 km of sediments (Lee et al., 1999). The acoustic basement is interpreted to consist largely of volcanic material that is overlain by thick layers of volcanic sill/flow sediment complexes in the northern part of the basin (Lee and Suk, 1998).

The Ulleung Basin is characterized by two distinct sedimentation patterns consisting mainly of mass-transport deposits (MTD) laid down during the late Neogene, and extensive turbidite and hemipelagic sedimentation since the Pleistocene (Riedel et al., 2012). During the late Neogene, slope failures caused by the regional deformation due to the back-arc closure, resulted in the widespread deposition of mass flow complexes in the basin (Riedel et al., 2012). Since the Pleistocene, and continuing on to the present, mass flow processes have rapidly shifted landward, forming debris aprons in the base-of-slope region, while turbidite and hemipelagic sedimentation has prevailed in the central basin. The southern part of the basin is characterized by slide or slump deposits (Lee and Suk, 1998; Lee et al., 1999; Chough et al., 2000).

III. ACQUISITION OF DOWNHOLE LOG DATA

For the purpose of gas hydrate exploration, LWD was conducted using the proprietary Schlumberger logging tools GeoVision, SonicVision, PowerPulse, and AdnVision on board the Fugro vessel RemEtive from 21 September to 11 October 2007. LWD data (i.e., natural gamma, resistivity, velocity, porosity, and density) were acquired from the seafloor to ~220 mbsf (meters below seafloor). Density porosity (density-derived porosity) was calculated from matrix density, formation bulk density, and fluid density (Asquith and Krygowski, 2004). The two LWD sites (UBGH1-1, UBGH1-14) were located on the southwestern flank of the Ulleung Basin in water depths of 1445 and 1354 m, respectively (Fig. 1).

IV. RESULTS AND DISCUSSION

1. Seismic Characteristics around Logged Ssites

Site UBGH1 is located in the western slope of the Ulleung Basin (Fig. 1). The site is characterized by high-amplitude bottom-simulating reflections (BSRs) (Fig. 2). Site UBGHB1-14 is located in the southern part of the Ulleung Basin (Fig. 1). Based on seismic data (Figs. 2 and 3), the logged sites in the southwestern part of the Ulleung Basin of the East Sea are generally characterized by MTDs and turbidite/hemipelagic sediments (THS). The upper sediments of the logged holes contain turbidite/hemipelagic sediments, whereas the middle and lower sediments are characterized by MTDs and/or a mixed type of MTD and THS. A strong and regionally extensive BSR occurs around the logged sites (Figs. 2 and 3). Generally, the BSR signature provides traditional evidence for gas hydrate and/or opal A/opal CT conversion within sediment layers (Berndt et al., 2004). The BSR typically runs parallel to the seafloor because of the stability condition for gas hydrate presence depending on temperature and pressure. The BSRs in the Ulleung Basin are likely related to the presence of gas hydrate (Yoo et al., 2008; Horozal et al., 2009), considering their depth (generally shallower than 200 mbsf).

As shown in Figs. 2 and 3, seismic features such as MTD,

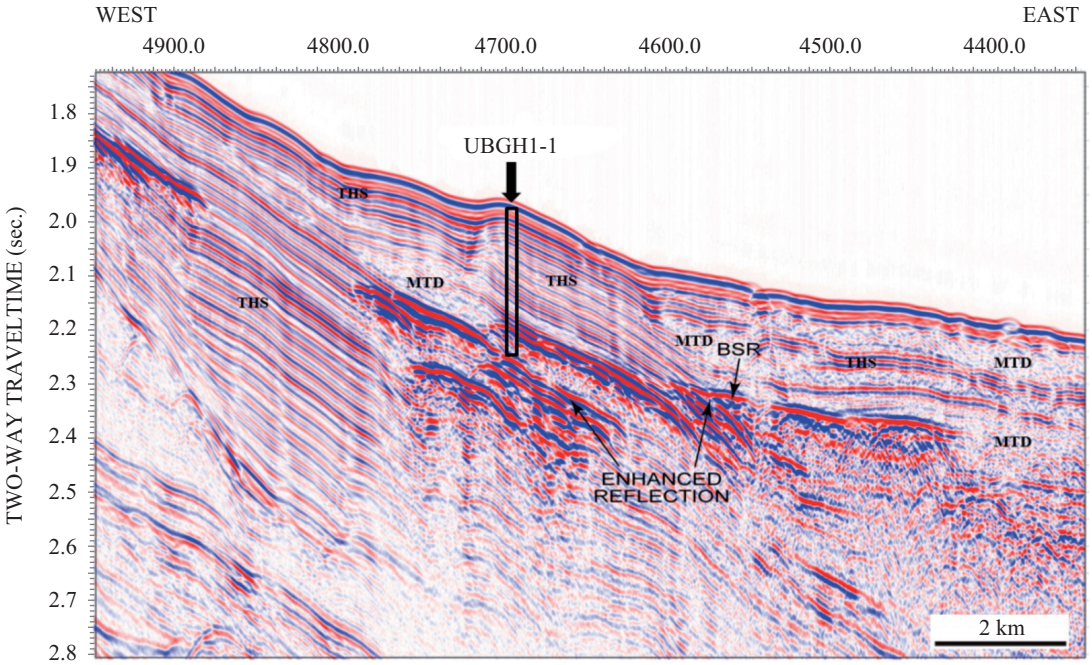

Fig. 2. East-west seismic profile through site UBGH1-1. The position of the bottom-simulating reflection (BSR) is indicated by arrows. Regional acoustic blanking above the BSR is also shown. Mass-transport deposits (MTD) are widely distributed. The drilled depth is approximately 220 mbsf (meters below seafloor).

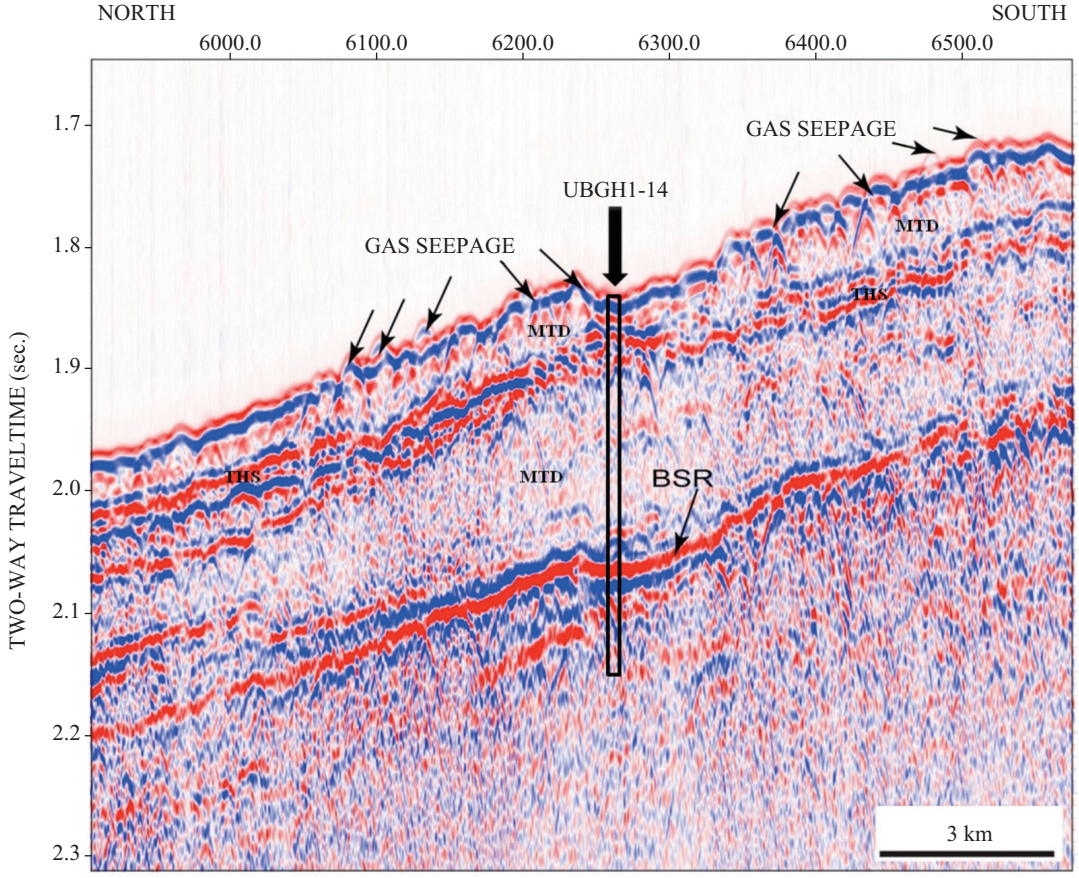

Fig. 3. South-north seismic profile through site UBGH1-14. The position of the BSR is indicated by arrows. Regional acoustic blanking above the BSR is also shown. Note that the MTD deposits are penetrated. The drilled depth is approximately 215 mbsf.

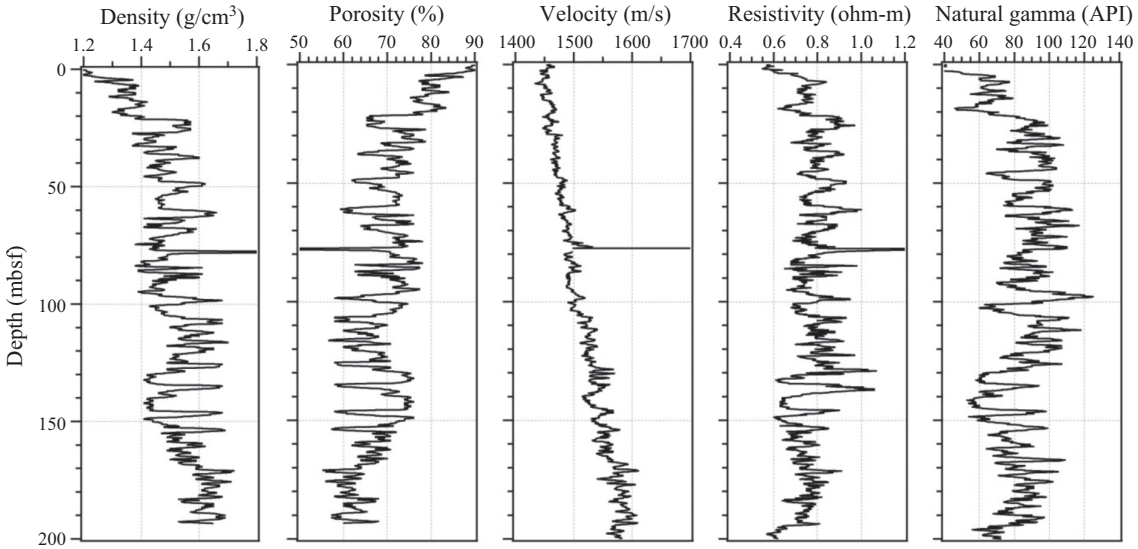

Fig. 4. Profile of physical properties at site UBGH1-1. Note high peak at 77 mbsf. Velocity constantly increases with depth. Note the considerable variation in physical properties with burial depth.

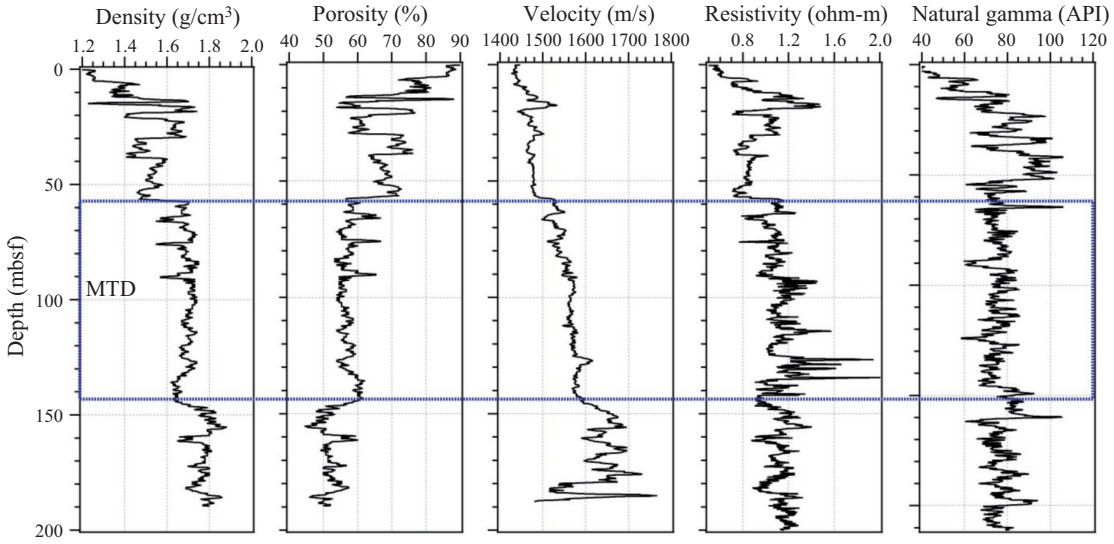

Fig. 5. Profile of physical properties at site UBGH1-14. The thick MTD is apparent in the profile. Note the low velocity around 180 mbsf.

THS, and BSR occur widely through the Ulleung Basin (Yoo et al., 2008; Horozal et al., 2009). Kim et al. (2011) reported that the physical properties of MTD in the Ulleung Basin are different from those of THS. The hemipelagic sediments in the study area most likely derived from the southern upper slope and shelf area (further away to the south of site UBGH1-14) and extended to the basin plain during the Quaternary. These processes are mostly responsible for gravity mass transport features, such as slides, slumps, debris-flows, and turbidity current (Lee et al., 1996).

In addition to sites UBGH1-1 and UBGH1-14 (Figs. 2 and 3), enhanced reflections below the BSR are identified at many other locations in the Ulleung Basin. These are likely caused by strong acoustic impedance contrasts due to the presence of free gas (Holbrook et al., 1996; Wood and Ruppel, 2000), which causes a distinct decrease in compressional wave velocity. Amplitude blanking within THS is also possible due to the presence of gas hydrate (Horozal et al., 2009). However, there was no direct evidence of this phenomenon in the log data. As shown in Fig. 3, gas seepages frequently appear on the seafloor of site UBGH1-14. These are probably responsible for the free gas escaping from seafloor sediments. In addition, the chaotic characteristics of the seafloor can be interpreted as the upper expression of a recent debris flow, which has not yet been buried and covered by smooth turbidite sediments.

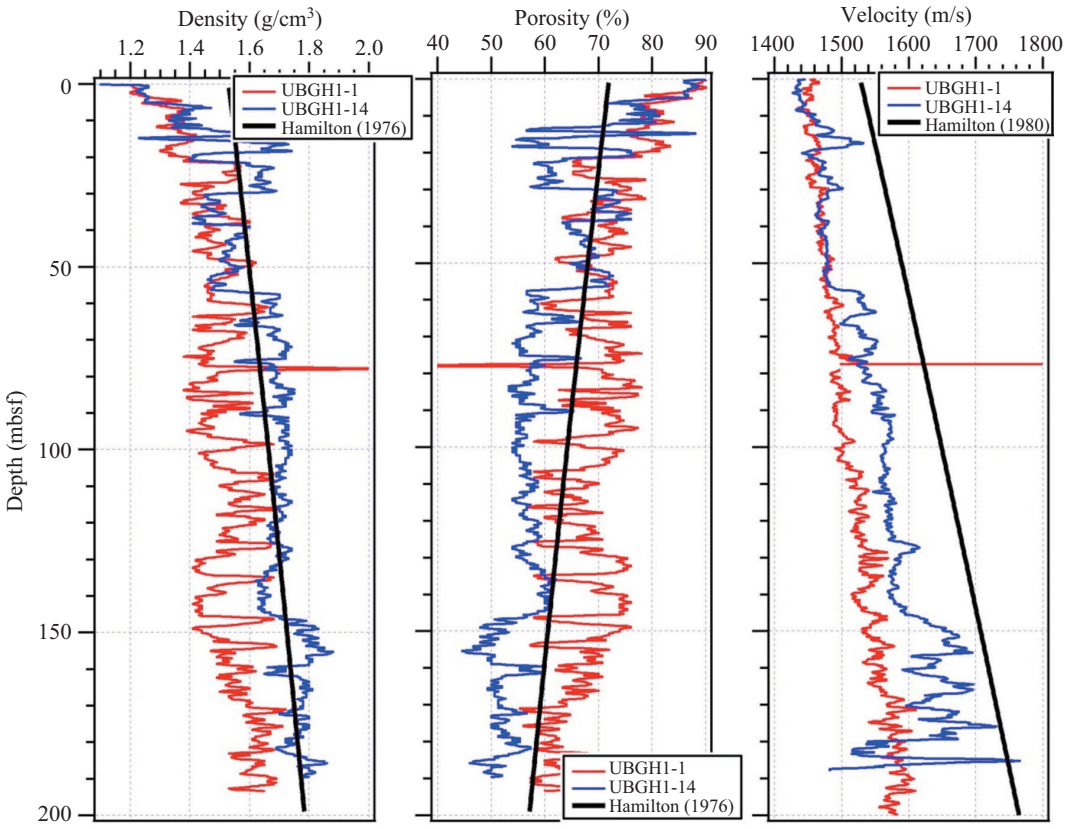

Fig. 6. Comparison of density, porosity, and velocity for the two sites. For comparison, Hamilton's curves (1976, 1980) are plotted as well.

2. Interpretation of Variations in Physical Properties with Depth

The depth variations of physical properties for the two sites are shown in Figs. 4 and 5. The greatest advantage of such log data is that they contain a relatively high-resolution and continuous record of the physical properties of the sediments in the logged hole. The density and porosity of site UBGH1-1 show increasing and decreasing patterns with high variation as depth increases (Fig. 4). The frequent variations are likely due to the difference in sedimentary environment and/or processes, caused by the repeated transition of the turbidite/hemipelagic sediment (THS) boundary (Fig. 2). Physical properties (e.g., porosity, density) of unconsolidated marine sediments are important variables contributing to sound velocity variation (Hamilton, 1970; Hamilton and Bachman, 1982). In general, lithological variability of recent unconsolidated marine sediments is described predominantly by changes in grain size distribution, which in turn is responsible for the variation of physical properties (Hamilton and Bachman, 1982; Richardson et al., 2002). Thus, the physical properties of recent sediments (mainly seafloor sediments) are likely to reflect the variation of sediment texture (e.g., mean grain size) rather than the effects of diagenesis (e.g., compaction and/or consolidation). However, porosity and water content generally decrease with burial depth as a result of dewatering by compaction and consolidation. As a result, the velocity of site UBGH1-1 increases linearly from 1450 to 1650 m/s with burial depth (Fig. 4). The resistivity and natural gamma signatures of site UBGH1-1 do not show distinct characteristics. The sharp peaks of density (> 1.8 g/cm^3), porosity (< 50%), velocity (> 1700 m/s), and resistivity (> 1.2 ohm·m) at approximately 77 mbsf are likely responsible for carbonate nodules, which sometimes appear within the sediments (KNOC, 2008).

The density and porosity of site UBGH1-14 show interesting patterns with sediment depth (Fig. 5). As shown in Fig. 5, the sediments above the MTD show significant variation with depth. The physical properties at the depth interval corresponding to MTD are characterized by a distinct boundary. At the interval between 15 and 30 mbsf, the high density (1.65-1.75 g/cm^3), velocity (> 1550 m/s), and resistivity (~1.5 ohm·m) values are likely attributable to the presence of sandy materials. Whereas at just above 15 mbsf, the low density, porosity, and gamma values and the high values of velocity and resistivity may be attributed to the presence of gas hydrate in the sediments. Within the MTD unit, the log data of high density (roughly 1.7 g/cm^3) and low porosity (< 60%) are almost constant throughout the MTD. The velocity increase ranges from slight to constant. Resistivity and natural gamma are constant relative to the upper sediments. This suggests that the sediments of the MTD may be formed by one sedimentary event. Beneath the MTD, the section is characterized by the

high values of density (> 1.8 cm^3) and velocity (~1750 m/s) and low porosity values (< 50%). Resistivity and natural gamma are relatively constant. Therefore, this may be considered the other MTD event, although the evidence for such an event is not clear in the seismic profile (Fig. 3). The abrupt drop (~1500 m/s) of velocity at 180 mbsf, despite the lack of significant variation of density and porosity, is likely due to free gas. Generally, small amounts of gas significantly decrease the compressional wave velocity (Wilkens and Richardson, 1998).

A comparison of sites UBGH1-1 and UBGH1-14 for density, porosity, and velocity is shown in Fig. 6. Hamilton (1976, 1980) reported the gradient of physical properties (e.g., density, porosity, velocity) with burial depth for various sediment types (e.g., calcareous sediment, diatomaceous and radiolarian ooze, pelagic clay, diatomaceous ooze, and terrigenous sediment) using a consolidation test and elastic rebound theory. Hamilton (1976, 1980) suggested that his model can be applied to terrigeneous shelf in the world ocean for similar texture and composition. In this study, the equation for terrigeneous sediment of Hamilton (1976, 1986) was applied for comparison. As shown in Fig. 6, the overall trends with burial depth are similar to those of Hamilton (1976, 1980). However, site UBGH1-14 shows higher density and lower porosity than those of Hamilton, likely owing to MTDs. In contrast, site UBGH1-1 is characterized by low density and high porosity relative to Hamilton's curve. Interestingly, the velocities of the two sites are significantly lower than those reported by Hamilton. One of the reasons for this is the presence of shallow gas and/or free gas related to gas hydrate dissociation in the sediments. Generally, site UBGH1-1 is characterized by more frequent depth variation compared with site UBGH1-14. As mentioned earlier, this is thought to be the reason for the differences in physical properties found in individual sediment layers as indicated by the repetition of turbidite sequences with burial depth, which in turn are likely due to differences in gradient with depth based on sediment types and/or sedimentary environment.

3. Relationships among Physical Properties

1) Velocity-Porosity

In unconsolidated marine sediments, the most important parameters controlling porosity are the size, shape distribution, mineralogy, and packing of the solid grains (Hamilton, 1970, 1980; Hamilton and Bachman, 1982). The velocity is largely determined by the effect of pore-water compressibility as opposed to that of the mineral solids (Hamilton, 1976, 1980). A cross plot of velocity-porosity is illustrated in Fig. 7. The relationship of velocity to porosity is particularly useful for distinguishing the consolidation state of sediment from the extent of diagenesis. In general, increasing consolidation in soft sediments tends to increase velocity through a decrease in porosity; whereas the cementation produces an increase in velocity through an increased rigidity of the sediment with little or no reduction in porosity (Dadey and Klaus, 1992).

Numerous studies have been conducted to determine a relationship between velocity and porosity for a variety of sediments and rock types. The curves of Wood (1941) and Wyllie et al. (1956) are shown for reference (Fig. 7). Wood's curve describes the relationship between velocity and porosity in clay sediments (i.e., no rigidity and in suspension). The Wyllie time-average equation has been most widely used as a function for describing sedimentary rocks having complete rigidity. This relationship is only reliable for consolidated sandstone over a small porosity range of 25% to 30% (Raymer et al., 1980). Thus, Wood and Wyllie's equations roughly define the lower and upper boundaries of velocity variation with porosity, respectively. The curve in Hamilton's (1970) study is also plotted for comparison (Fig. 7). The data from this study lies above the fitting line suggested by Wood (1941), and below Hamilton's curve. This is likely owing both to the sediment being finer than that used by Hamilton and to the sedimentary environment being different. Interestingly, the plotted data are clearly separated into two sites (Fig. 7), likely because of the above-mentioned differences in the physical properties each site. However, a general trend of decreasing velocity with increasing porosity is apparent, as would be expected in marine sediments.

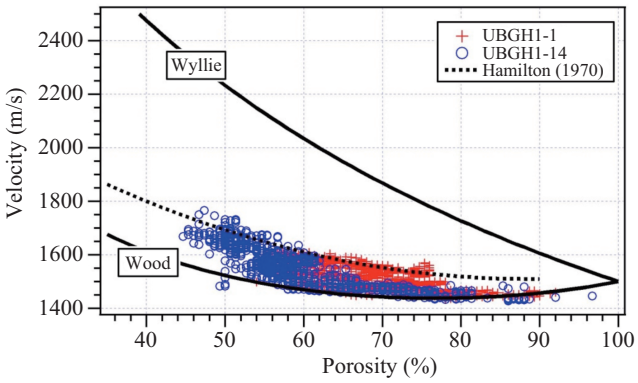

Fig. 7. Relationship between porosity and velocity. The curves of Wood (1941), Wyllie (1958), and Hamilton (1970) are plotted as well. Note the data clustering for each site.

2) Velocity-Density

The plot of velocity versus density is positively correlated (Fig. 8). However, sites UBGH1-1 and UBGH1-14 are separated on the plot, indicating a difference in their physical properties. Density can be affected by mineralogy, compaction, consolidation of sediment, and water content (Hamilton, 1970; Hamilton and Bachman, 1982). Thus, the velocity-density relationship for marine sediments is a function of mineral composition, subbottom depth, and depositional history. Therefore, the seismic velocity of marine sediment generally increases with increasing density. This result follows the general pattern as well as Hamilton's curve, although Hamilton's line lies above the curve of our data within the range of low densities and velocities.

3) Velocity-Resistivity

Velocity also has a positive relationship with resistivity,

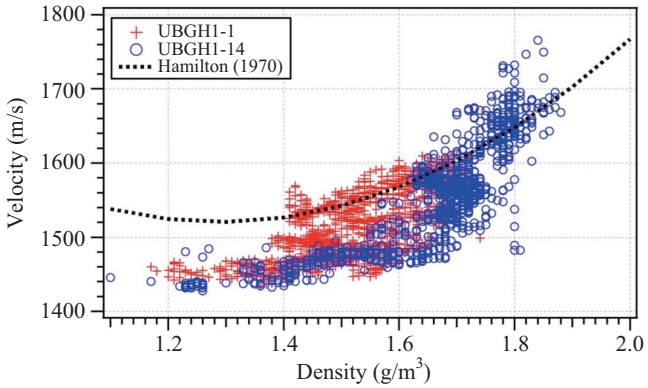

Fig. 8. Relationship between density and velocity. Hamilton's curve is plotted for reference.

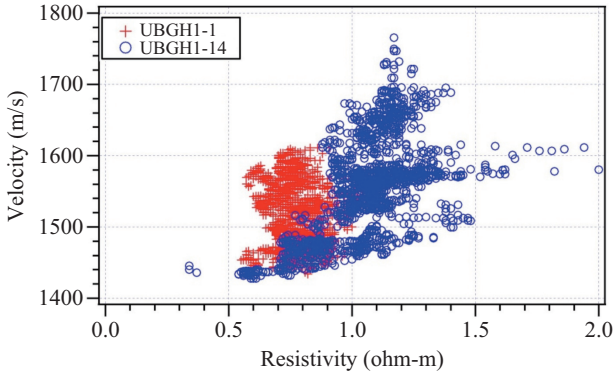

Fig. 9. Relationship between resistivity and velocity. Note the data clustering for each site.

showing increasing velocity with increasing resistivity (Fig. 9). However, there is considerable scattering of data, which is clearly separated by each site, indicating different physical property. UBGH1-1 is characterized by one cluster, indicating no significant change in physical properties. In contrast, site UBGH1-14 shows severe scattering and three clusters. This may suggest that the physical properties of site UBGH1-14 can be grouped according to differences in the sediment properties. As mentioned earlier, this site is characterized by MTD, and results in a variation of sediment properties. Generally, electrical resistivity for unconsolidated marine sediment is the range of 1.0 to 1.5 ohm·m (mostly < 1 ohm·m) in the upper 300 mbsf (Hyndman et al., 1999), caused by seawater saturation of porous sediments. However, the value can be increased with a significant change in the physical properties by sediment diagenetic processes such as silica diagenesis (Nobes et al., 1992; Kim et al., 2007). In addition, gas hydrate has a high resistivity (Hyndman et al., 1999; Collett and Ladd, 2000; Kim et al., 2011, 2013), and free gas also increases resistivity. Nonetheless, although this site is located within a gas hydrate occurrence zone, the hydrate does not seems to significantly affect physical properties other than velocity.

4. Frequency Distribution of Physical Properties

Frequency distributions of density, velocity, and natural gamma ray measurements from sites UBGH1-1 and UBGH1-14 are shown in Fig. 10. The distribution patterns of each property are obviously different. The density distribution at site UBGH1-1 ranges mainly from 1.4 to 1.7 g/cm^3. Site UBGH1-14 shows 1.65 to 1.8 g/cm^3. Velocity also has different frequency distributions. Site UBGH1-14 is characterized by frequency distributions of higher velocity (> 1600 m/s) than site UBGH1-1 (mostly < 1600 m/s). In the case of natural gamma, site UBGH1-1 has close to a normal distribution (mainly 50-120 API). Site UBGH1-14 shows a narrow normal distribution pattern (mainly 60-100 API), indicating changes in the physical properties caused by differences in sedimentary environment and processes as well as the presence of MTD. As described above, the MTD at site UBGH1-14 is thicker than that of site UBGH1-1. High values of density, velocity, and resistivity and low values of porosity are observed in the MTD.

CONCLUSIONS

The upper sediments of logged sites are dominated by turbidite/hemipelagic sediments, whereas the lower sediments are characterized by mass transport deposits. Based on physical properties, site UBGH1-1 appears to have been most affected by consolidation/compaction effects and the type of sediment. In addition, frequent variations in physical properties with depth at site UBGH1-1 are likely attributable to repeated turbidite sequences. At site UBGH1-14, MTD significantly affected

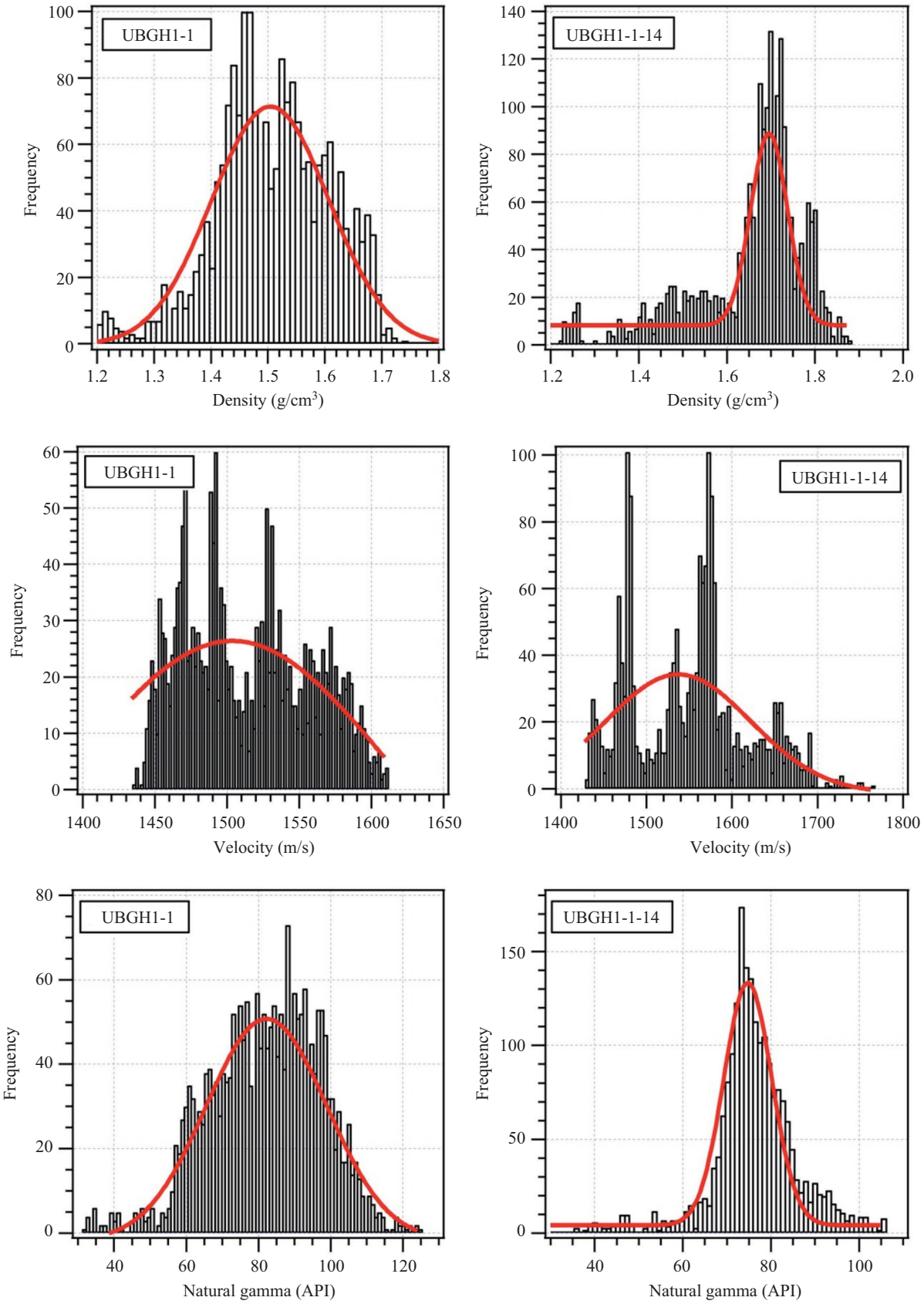

Fig. 10. Frequency distribution of density, velocity, and natural gamma at sites UBGH1-1 and UBGH1-14. In this comparison, the data of site UBGH1-14 deviate from a normal distribution.

the variability of physical properties. Exceptionally, free gas produced during the dissociation of gas hydrate was responsible for low velocities. The overall relationships between physical properties follow general patterns of marine sediments, but some data scattering and clustering occurred for each site exist. This can be interpreted to be the result of differences in the sediment properties caused by mass flow deposits. Additionally, the frequency distribution of physical properties for the two sites likely reflects the differences in depositional environments.

ACKNOWLEDGMENTS

This work was supported by Ministry of Knowledge Economy (MKE) and the Gas Hydrate Research and Development Organization (GHDO) of Korea. We gratefully thank the participants of the UBGH1 Program. This research is affiliated with the K-IODP project, the "International Ocean Discovery Program", funded by the Ministry of Oceans and Fisheries, Korea.

REFERENCES

Asquith, G. and D. Krygowski (2004). Petrophysical techniques. Basic well log analysis: AAPG Methods in Exploration 16, 137-149.

Berndt, C., C. Bunz, T. Clayton, T. Mienert and M. Saunders (2004). Seismic character of bottom simulating reflectors: examples from the mid-Norwegian margin. Marine and Petroleum Geology 21, 723-733.

Chough, S. K., H. J. Lee and S. H. Yoon (2000). Marine Geology of Korean Seas, second edition, Elsevier, Amsterdam, 313.

Collett, T. S. and J. Ladd (2000). Detection of gas hydrate with downhole logs and assessment of gas hydrate concentrations (saturation) and gas volumes on the Blake Ridge with electrical resistivity log data. Proceedings of the Ocean Drilling Program, Scientific Results 164, 179-191.

Dadey, K. A. and A. Klaus (1992). Physical properties of volcaniclastic sediments in the Izu-Bonin Area. In: Taylor, B; Fujioka, K; et al. (eds.), Proceedings of the Ocean Drilling Program, Scientific Results, College Station, TX (Ocean Drilling Program), 126, 543-550.

Hamilton, E. L. (1970). Sound velocity and related properties of marine sediments, North Pacific. Journal of Acoustical Society of America 75, 4423-4446.

Hamilton, E. L. (1980). Geoacoustic modeling of the seafloor. Journal of Acoustical Society of America 68, 1313-1340.

Hamilton, E. L. and R. T. Bachman (1982). Sound velocity and related properties of marine sediments. Journal of Acoustical Society of America 72, 1891-1904.

Holbrook, W. S., H. Hoskins, W. T. Wood, R. A. Stephen, D. Lizarralde and Leg 164 Science Party (1996). Methane hydrate and free gas on the Blake Ridge from vertical seismic profiling, Science 273, 1840-1843.

Horozal, S., G. H. Lee, B. Y. Yi, D. G. Yoo, K. P. Park, H. Y. Lee, W. S. Kim, H. J. Kim and K. S. Lee (2009). Seismic indicators of gas hydrate and associated gas in the Ulleung Basin, East Sea (Japan Sea) and implications of heat flows derived from depths of the bottom-simulating reflector. Marine Geology 258, 126-138.

Hyndman, R. D., T. Yuan and K. Morgan (1999). The concentration of deep sea gas hydrates from downhole electrical resistivity logs and laboratory data. Earth Planetary Scientific Letter 172, 167-177.

Kim, G. Y., D. G. Yoo, H. Y. Lee, Y. J. Lee and D. C. Kim (2007). The relationship between silica diagenesis and physical properties in the East/Japan Sea: ODP Legs 127/128. Journal of Asian Earth Sciences 30, 448-456.

Kim, G. Y., B. Y. Yi, D. G. Yoo, B. J. Ryu and M. Riedel (2011). Evidence of gas hydrate from downhole logging data in the Ulleung Basin, East Sea. Marine and Petroleum Geology 28, 1979-1985.

Kim, G. Y., B. Narantsetseg, B. J. Ryu, D. G. Yoo, J. Y. Lee, H. S. Kim and M. Ridel (2013). Fracture orientation and induced anisotropy of gas hydrate-bearing sediments in seismic chimney-like structures of the Ulleung Basin, East Sea. Marine and Petroleum Geology 47, 182-194.

KNOC (2008). Investigation of gas hydrate exploration UBGH1 Ulleung Basin, East Sea, offshore Korea. Fractual Field Report (Report No. 0201-6242), Gyeonggi-do, Korea.

Lee, H. J., S. K. Chough and S. H. Yoon (1996). Slope stability change from late Pleistocene to Holocene in the Ulleung Basin, East Sea (Japan Sea). Sedimentary Geology 104, 39-51.

Lee, G. H., H. J. Kim, M. C. Suh and J. K. Hong (1999). Crustal structure, volcanism and opening mode of the Ulleung Basin, East Sea (Sea of Japan), Tectonophysics 308, 503-525.

Lee, G. H. and B. C. Suk (1998). Latest Neogene-Quaternary seismic stratigraphy of the Ulleung Basin, East Sea (Sea of Japan). Marine Geology, 146, 205-224.

Nobes, D. C., R.W. Murray, S. I. Kuramoto, K. A. Pisciotto and P. Holler (1991). Impact of silica diagenesis on physical variation. In: Pisciotto, K. A., Ingle Jr., J. C., von Breymann, M. T., Barron, J. (eds.), Proceedings of the Ocean Drilling Program, Scientific Results. 127/128. Part 1, College Station, Texas Ocean Drilling Program, 3-31.

Raymer, L. L., E. R. Hunt and J. S. Gardner (1980). An improved sonic transit time-to-porosity transform. Trans. SPWLA Annu. Logging Symp., 21st: P1-P13.

Richardson, M. D., K. B. Briggs, S. J. Bentley, D. J. Walter and T. H. Orsi (2002). The effects of biological and hydrodynamic processes on physical and acoustic properties of sediments off the Eel River, California. Marine Geology 182, 121-139.

Riedel, M., J. J. Bahk, N. A. Scholz, B. J. Ryu, D. G. Yoo, W. S. Kim and G. Y. Kim (2012). Mass-transport deposits and gas hydrate occurrences in the Ulleung Basin, East Sea-Part 2: Gas hydrate content and fracture-induced anisotropy. Marine and Petroleum Geology 35, 75-90.

Rider, M. H. (1990). Gamma-ray log shape used as facies indicator: critical analysis of an oversimplified methodology. Geological Society Special Publication 48, 27-37.

Russell, W. L. (1941). Well logging by radioactivity. Bulletin of the American Association of Petroleum Geologists 9, 1768-1788.

Wilkens, R. H. and M. D. Richardson (1998). The influence of gas bubbles on sediment acoustic properties: in situ, laboratory, and theoretical results from Eckernforde Bay, Baltic Sea. Continental Shelf Research 18, 1859-1892.

Wood, A. B. (1941). A textbook of sound. London: G. Bell and Sons.

Wood, W. and C. Ruppel (2000). Seismic and thermal investigations of hydrate bearing sediments on the Blake Ridge Crest: a synthesis of ODP Leg 164 results. Proc. Ocean Drill. Program. Final Report 164, 253-264.

Wyllie, M. R. J., A. R. Gregory and G. H. F. Gardner (1956). Elastic wave velocities in heterogeneous and porous media. Geophysics 21, 41-70.

Yoo, D. G., D. H. Kang, N. H. Koo, W. S. Kim, G. Y. Kim, S. H. Chung, Y. J. Kim, H. Y. Lee, K. P. Park, G. H. Lee and S. C. Park (2008). Geophysical evidence for the occurrence of gas hydrate in the Ulleung Basin, East Sea. Journal of the Geological Society of Korea 44, 645-655.